## **CONFERENCE PRE-PRINT**

# GLOBAL FLUID TURBULENCE SIMULATIONS OF PEDESTAL RELAXATION EVENTS IN THE I-MODE REGIME WITH GRILLIX

CHRISTOPH PITZAL
Max Planck Institute for Plasma Physics,
Garching, Germany
Email: christoph.pitzal@ipp.mpg.de

ANDREAS STEGMEIR, TIM HAPPEL, KAIYU ZHANG, KONRAD EDER WLADIMIR ZHOLOBENKO, PHILIPP ULBL, MANUEL HERSCHEL, FRANK JENKO Max Planck Institute for Plasma Physics, Garching, Germany

### **Abstract**

In the paper, trans-collisional fluid turbulence simulations of the Pedestal Relaxation Events (PREs) in the improved energy confinement mode (I-mode) regime with GRILLIX are presented. Within 5 ms of simulation time, three PREs are observed in the GRILLIX simulation, which recover a wide range of experimentally observed characteristics of PREs. It is shown that the PREs are caused by internal dynamics and are not triggered by, e.g. the boundary conditions. PREs manifest as periodic energy ejections similar to Edge Localised Modes (ELMs). Although both events feature intermittent bursts, the underlying mechanism seems to be very different. While ELMs are triggered by Peeling-Ballooning modes, which become unstable in the steep-gradient region of the pedestal, the underlying mechanism for the PREs present in the GRILLIX simulations are Micro-Tearing-Modes (MTMs). The present mode was identified as a MTM by detailed analysis of various mode properties. The most clear fingerprints are the observed tearing parity for the electrostatic and the parallel magnetic vector potential in radial direction and the dispersion relation computed from the simulation data, which matches nicely the linear kinetic estimate. Furthermore, the gradient lengths of electron temperature and density are analysed over time during the simulation and compared to a linear estimate for the growth rate of the employed fluid model, which is in excellent agreement. Based on all these analyses, a global mechanism underlying PRE cycles is proposed.

# 1. INTRODUCTION

Investigating reactor-relevant operational scenarios for potential future fusion power plants is a task of major importance for the whole fusion community. One such operational scenario is the improved energy confinement mode (I-mode), which features elevated energy confinement time, low impurity content and the absence of Type-I Edge Localised Modes (ELMs) [1, 2]. However, when the operational point moves close to the I-H transition, Pedestal Relaxation Events (PREs) are observed in experiments in ASDEX Upgrade and Alcator C-mod [3]. A similar phenomenon is also observed in EAST [4]. PREs cause periodically occurring and short-lasting increases of radial heat transport, similar to ELMs. Type-I ELMS are triggered by Peeling-Ballooning modes in the pedestal and can cause ejections of up to 10 % of the stored energy [5]. PREs are a lot less violent and eject at most about 1 % of the plasma stored energy [6] and also the underlying mechanism is expected to be very different. Simulations of the edge conditions in I-mode with a fluid model is very challenging because of the low collisionality, which is present in the plasma edge of a fusion device ( $\rho_{\rm pol} > 0.9$ ). The edge turbulence fluid code GRILLIX [7] was extended for low collisionalities by the implementation of a Landau-fluid closure for the parallel conductive heat fluxes [8].

With this extension, GRILLIX is used to investigate PREs with fluid turbulence simulations performed with the parameters of the ASDEX Upgrade I-mode discharge # 37980. Within the simulation time of 5 ms, we observe three PREs. These PREs are able to recover a wide range of experimentally observed characteristics of PREs, e.g. they affect mainly the electron temperature profile, they show increased magnetic activity and the duration of the PRE of 0.3 ms matches very well [6]. By collecting fingerprints of the mode present in the simulation during the PRE, which includes tearing parity visible in the electrostatic potential and the parallel magnetic vector

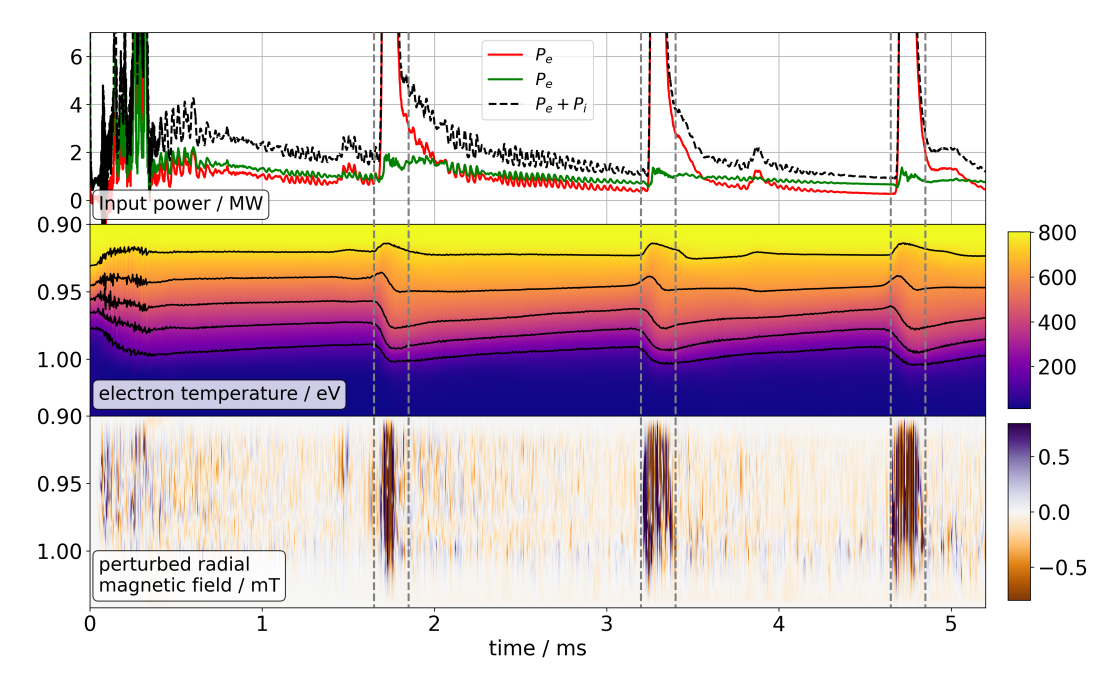


FIG. 1. Time trace of input power, electron temperature and perturbed radial magnetic field, the latter two plotted over  $\rho_{\text{pol}}$  at the OMP. The three PREs are marked with grey dotted lines.

potential, predominantly radial electromagnetic electron heat transport and the dispersion relation computed from the simulation data matching nicely the linear kinetic estimate [9]. The MTM, which is observed during the PRE, is located at the outboard midplane (OMP) around  $\rho_{\rm pol}=0.95$ . We observe that the electron temperature gradient is flattened after the PRE at this location, which should decrease the drive for MTMs. To follow this observation in more detail, we analyse the electron temperature and density gradient lengths at this position over time for our simulation. The path taken by the system in this gradient length space is compared to the growth rate calculated in a linear estimate for our fluid model, which agrees nicely with the behaviour of the full non-linear system. We also investigate the influence of the recently implemented Landau-fluid closure on the results by comparing them to a simulation with the previously used Braginskii closure with additionally applied free-streaming heat-flux limiters [8]. The Braginskii simulation produces a quiescent simulation without any major intermittent events and shows no typical I-mode features, like the pedestal in electron temperature.

## 2. TURBULENCE SIMULATION

The setup of the simulation is based on the ASDEX Upgrade (AUG) discharge # 37980, which is performed in unfavourable configuration (upper-single null). The time point  $t=4.1\,\mathrm{s}$  of the discharge is considered, where a stationary I-mode is observed. The magnetic field is  $B=2.5\,\mathrm{T}$  on axis. The plasma is heated by electron-cyclotron-resonance heating and by neutral-beam injection. After subtracting the radiation losses  $P_{\rm rad}$ , which are not modelled by GRILLIX, the input power is ca.  $1.9\,\mathrm{MW}$ . For this simulation, we used 16 poloidal. The grid distance is constant with a value of  $1.45\,\mathrm{mm}$  within a plane. The values at the inner core boundary of  $n(\rho_{\rm pol}=0.91)=3.8\cdot10^{19}\,\mathrm{m}^{-3}$ ,  $T_e(\rho_{\rm pol}=0.91)=800\,\mathrm{eV}$  and  $T_i(\rho_{\rm pol}=0.91)=500\,\mathrm{eV}$  are taken from the experimental measurements, see fig. 2. The boundary conditions near the core are imposed using adaptive sources. These sources are active between  $\rho_{\rm pol}=0.90-0.91$  and they inject particles and heat to keep the values of n,  $T_e$  and  $T_i$  close to the target values. The input of heating power and particles is tracked over the simulation. At the divertor target sheath boundary conditions with sheath transmission factors of  $\gamma_{sh,e}=1.0$  and  $\gamma_{sh,i}=0.1$  are applied. For a more detailed description of the boundary conditions, we refer to [8]. The presented simulation uses the same physical model as the simulation in [8], i.e. a drift-reduced electromagnetic Braginskii model including trans-collisional extensions. These extensions are a neoclassical ion viscosity and a Landau-fluid closure for parallel heat fluxes. The previously used one-moment neutral gas model is replaced by a three-moment model [10].

For an overview of the simulation, a time trace of input power and of the OMP profiles of electron temperature and perturbed radial magnetic field is provided in fig. 1. We observe three intermittent bursts marked by grey dotted lines. During these bursts, the heating power increases significantly, mainly for the electron input power  $P_e$ . During the three events, we also see strong magnetic activity in the radial perturbed magnetic field and a

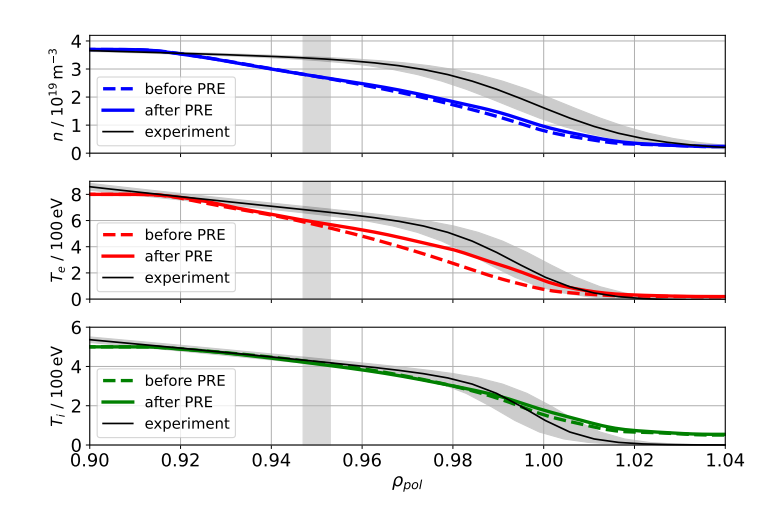


FIG. 2. OMP profiles of density, electron and ion temperature before and after the PRE. And the experimental measurements. The region around  $\rho_{\text{Dol}} = 0.95$  where the MTM is centered and is marked in grey

significant effect on the electron temperature profile.

The characteristics of the three intermittent events in the simulation are in line with experimentally observed PRE properties. In experiments, PREs mainly flatten the electron temperature profile rather than the density profile [6]. Furthermore, when a PRE occurs, strong magnetic activity is observed [3]. The duration of a PRE in our simulation of ca. 0.3 ms is very close to the duration observed in the experiment [6]. To show the effect of the PREs in our simulation in detail, the density, electron and ion temperature profiles are plotted before and after the second PRE in fig. 2. We see again that mainly the electron temperature profile is affected. In contrast to the experiment, the electron temperature is increased in the whole domain after the PRE, visible in fig. 2. We can explain this by taking a look at the adaptive sources near the core boundary. The radial transport in the simulation domain is increased by the PRE. The adaptive sources try to maintain the target value and increase the injected power. This means the boundary conditions are responsible for lifting the electron temperature profile during the PRE. We can make sure that internal dynamics are responsible for the PREs in our simulation, and they are not artificially induced by the boundary conditions. Therefore, we look at the causality of events. By taking a look at fig.1 again, more specifically at the second PRE. Here, we observe that first, the electron temperature profile flattens. When this perturbation reaches the region where the adaptive source is active, the input power for electrons  $P_e$  increases strongly in order to keep up the core value. The mode responsible for causing an increased radial transport appears around  $\rho_{pol} = 0.95$ . At this radial position, the electron temperature gradient flattens due to the PRE, which is visible in fig. 2 for  $T_e$  before and after the PREs, just like in the experiment.

## 3. PRES CAUSED BY MTMS

This section aims to prove that the microinstability underlying PREs in our simulation is a MTM. The first finger-print is that mainly the radial electron heat transport increases. Further analysis shows that this radial electron heat transport is primarily electromagnetic transport, so caused by magnetic flutter. The second fingerprint is found by investigation of the structure of the fluctuating magnetic vector potential  $\tilde{A}_{\parallel}$  and the fluctuating electrostatic potential  $\tilde{\phi}$  during a PRE. Their structure is shown in fig. 3. The mode in  $\tilde{A}_{\parallel}$  peaks at the OMP around  $\rho_{\rm pol}=0.95$ . The eigenfunctions of tearing modes extend in the radial direction [11]. We observe even parity in  $\tilde{A}_{\parallel}$  and odd parity in  $\tilde{\phi}$ . This combination is called tearing parity and is a distinct feature of tearing modes, such as MTMs [9]. The gobal three-dimensional structure of  $\tilde{A}_{\parallel}$  is shown in fig. 5.

The last fingerprint to mention here is the dispersion relation, calculated for  $\tilde{A}_{\parallel}$  on the flux surface  $\rho_{\rm pol}=0.95$  during the second PRE and shown in fig. 4. This radial position  $\rho_{\rm pol}=0.95$  was taken, because of the centre of the mode in  $\tilde{A}_{\parallel}$ . The computed dispersion relation shows a mode propagating in electron diamagnetic direction in the plasma frame. Furthermore, the mode is in excellent agreement with the frequency predicted by the analytical dispersion relation derived from linear kinetic estimates [9]. The peak of the mode is at  $k_y \rho_s = 0.2$ . With this list of fingerprints, we are able to state confidently, that the mode present in our simulation during the PREs is a MTM indeed.

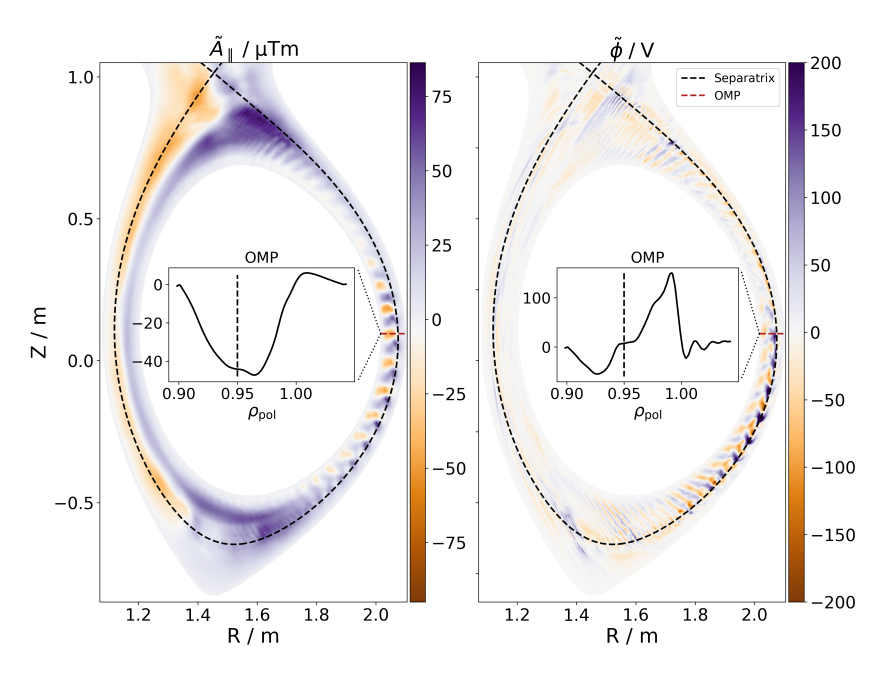


FIG. 3. Tearing parity which is visible for the fluctuating electrostatic potential  $\tilde{\phi}$  and the fluctuating magnetic vector potential  $\tilde{A}_{\parallel}$  in the radial direction at the OMP.

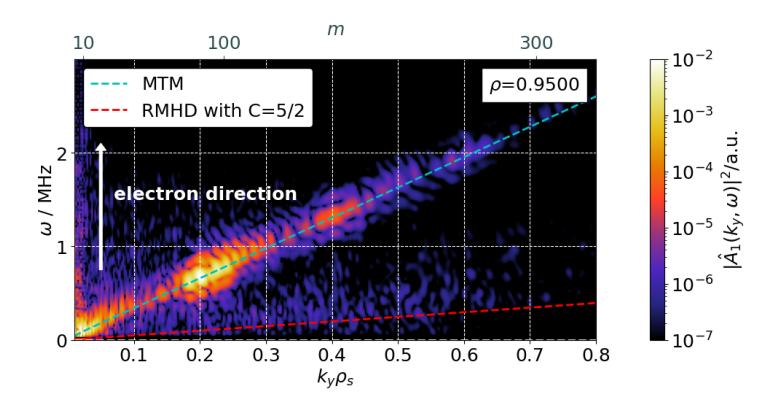


FIG. 4. Dispersion relation during a PRE indicating the underlying instability to be MTM

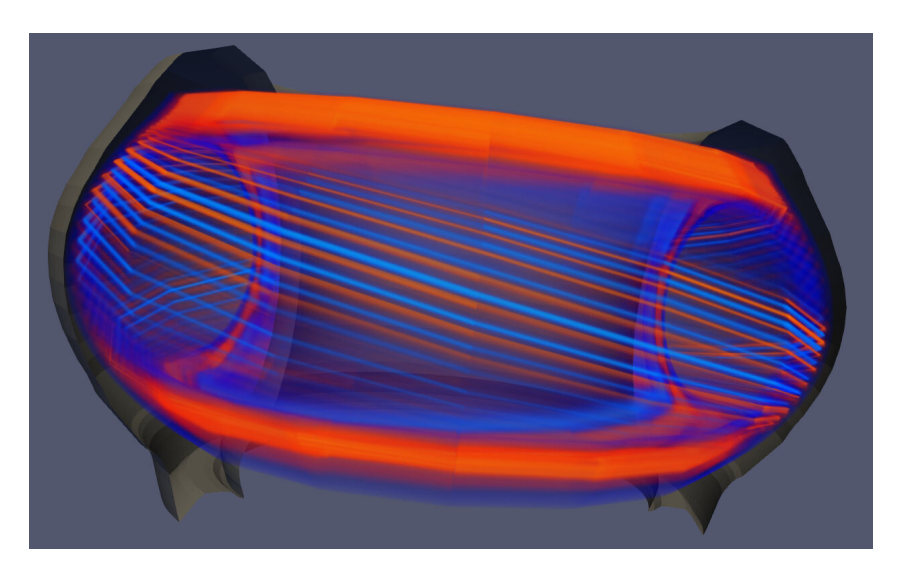


FIG. 5. 3D structure of the parallel magnetic vector potential  $A_{\parallel}$  during a PRE

## 4. SUMMARY AND OUTLOOK

In the manuscript, we presented global trans-collisional plasma fluid simulations performed with GRILLIX. They show intermittent bursts, which are linked to PREs. The simulation could reproduce key features of PREs observed in experiments. The underlying microinstability responsible for PREs in the simulation could be pinpointed to MTMs. The PREs in our simulation capture a range of experimentally observed characteristics, e.g. an increased magnetic activity during the PRE, mainly radial electron heat transport, and a match in the duration of PREs in comparison to the experiment. Therefore, we are confident that the presented PREs in the simulation are in good agreement with PREs in fusion experiments.

The fluid model, that was used here, shows certain limitations for low collisionality. For future investigations of the I-mode regime, either for steady-state or addressing PREs, the trans-collisional fluid model within GRILLIX should be improved, or higher fidelity models like the gyrokinetic code GENE-X [12] should be used.

## REFERENCES

- [1] WHYTE, D., et. al., Nuclear Fusion, vol. 50, no. 10, p. 105005, (2010)
- [2] HAPPEL, T., et al., Plasma Physics and Controlled Fusion, vol. 59, no. 1, p. 014004, (2016)
- [3] SILVAGNI, D., et al., Nuclear Fusion, vol. 62, no. 3, p. 036004, (2022)
- [4] ZHONG, X.M., et al., Nuclear Fusion, vol. 62, no. 6, p. 066046, (2022)
- [5] HUIJSMANS, G.T.A., et al., Physics of Plasmas, vol. 22, no. 2, (2015)
- [6] SILVAGNI, D., et al., Nuclear Fusion, vol. 60, no. 12, p. 126028, (2020)
- [7] STEGMEIR, A., et al., Physics of Plasmas, vol. 26, no. 5, p. 052517, (2019)
- [8] PITZAL, C., et al., Physics of Plasmas, vol. 30, no. 12, p. 122502, (2023)
- [9] HATCH, D., et al., Nuclear Fusion, vol. 61, no. 3, p. 036015, (2021)
- [10] EDER, K., et al., Plasma Physics and Controlled Fusion, vol. 67, no. 6, p. 065034, (2025)
- [11] HAZELTINE, R.D., et al., Physics of Fluids, vol. 18, no. 12, p. 1778-1786, (1975)
- [12] MICHELS, D., et al., Computer Physics Communications, vol. 264, p. 107986, (2021)